Journal of Applied Electrochemistry **30**: 43–48, 2000.

Performance evaluation of porous electrocatalysts via normalization of the active surface

J.P. IÚDICE DE SOUZA[1,3], T. IWASITA[1], F.C. NART[1] and W. VIELSTICH[2,4]
[1]*Instituto de Química de São Carlos, Universidade de São Paulo C.P. 780, 13560-970 São Carlos, Brazil;*
[2]*Institut für Physik, Universität der Bundeswehr München, Werner-Heisenberg-Weg 39, 85577 Neubiberg, Germany;*
[3]*On leave from: Departamento de Química, Universidade Federal do Pará, Rua Augusto Correa S/N, Belém, Pará, Brazil;*
[4]*Present address: Instituto de Química de São Carlos, Universidade de São Paulo, C.P. 780, 13560-970 São Carlos, Brazil*

Received 26 February 1999; accepted in revised form 15 June 1999

Key words: methanol electrooxidation, normalization of porous surfaces, PtRu catalysts

Abstract

When comparing the rate of electrochemical processes at different porous electrocatalysts a surface normalization should be used. It is shown for the case of methanol oxidation at PtRu layers electrodeposited on gold substrates that substantially different data are obtained for current, mass spectrometry signals and integrated IR band intensities of the products, with and without normalization of the catalyst surface used. Using stripping of saturated CO coverage as a normalization tool, cyclic voltammograms, on line MS and *in situ* FTIR spectroscopy give reasonable agreement of catalytic activity towards methanol oxidation.

1. Introduction

In comparing different electrocatalysts with respect to their effect on reaction rates, it must be ensured that data obtained refer to the same number of reactive surface sites. In many fundamental investigations this condition can easily be fulfilled as, for example, when using well-prepared single crystals surfaces [1, 2]. For smooth polycrystalline metals or alloys [3, 4] the problem may not be critical if caution is taken that the roughness factors of the surfaces remain low. The other extreme is large area electrodes as used in technical electrolysis and also in fuel cells stacks. The practical interest in this case is concentrated on the rate of reaction per amount of catalyst used, for example, in mA per mg noble metal [5, 6].

In the field of applied electrocatalysis a large number of studies have focused on the optimization of structure and composition of porous active surfaces [7–10]. Depending on the preparation procedure, samples of different composition, basically prepared according to the same method, may differ in their effective surfaces by more than a factor of two. In such a case the catalytic activities can only be compared if the experimental data are normalized to the respective effective surface. Typical examples are studies on the performance of large area porous electrodes as used for fuel cells operating with liquid fuels. Of special interest is the search for a catalyst suitable for methanol oxidation. In this case, several binary catalysts such as PtRu [11–13], PtRh [14, 15], PtSn [14, 16], $PtWO_3$ [17], PtMo [18, 19], and also ternary systems [20, 21], have been compared. The preparation procedure, either codeposition or sputtering of the metal components, normally results in a high surface roughness. In some cases technical porous electrodes of particularly large real area have been used [22].

In this work we intend to show, by using codeposited PtRu layers of different metal compositions for the electrooxidation of methanol as an example, that for correct comparison of data, surface normalization is essential. The stripping of saturated CO adlayers is used to normalize three rate dependent parameters: the oxidation current, the formation of CO_2 as measured via online mass spectrometry (DEMS) [23] and *in situ* FTIR spectroscopy [24]. It must be emphasized that in the case of PtRu deposits the determination of the real surface area by stripping of a hydrogen adlayer is not a suitable alternative. In this case, due to the strong adsorption of CO on PtRu, saturated CO adlayers can be used as a measure for the active surface.

2. Experimental details

2.1. *Electrodes*

A reversible hydrogen electrode (RHE) in the electrolyte solution and a platinized Pt foil were used as reference and counter electrode, respectively. For FTIR measurements, the working electrodes were obtained by potent-

iostatic deposition of Pt or codeposition of Pt and Ru onto a smooth Au substrate (a disc of 0.38 cm^2 geometric area, previously polished to a mirror finishing). For DEMS the electrodeposits were made on a gold layer (1.13 cm^2 area, 50 nm thickness) prepared by gold sputtering onto a SCIMAT® membrane (thickness 60 μm, mean pore size 0.17 μm, 50% porosity). All electrodepositions were performed in a 1 M $HClO_4$ solution containing the appropriate amount of Pt and Ru salts for 5 min at 0.2 V vs RHE.

The atomic bulk compositions of the electrodeposited electrodes were measured by EDAX (energy dispersive analysis of X-rays) and are listed in Table 1.

2.2. *Chemicals, solutions*

Solutions were prepared with Millipore-MilliQ® water and analytical grade $HClO_4$ acid (Merck), methanol (Merck), $H_2PtCl_6.6\,H_2O$ (Aldrich) and $RuCl_3.3\,H_2O$ (Aldrich). The CO 99.9 and N_2 5.0 were used.

2.3. *FTIR measurements*

FTIR spectra were obtained with a Brucker IFS 66 spectrometer provided with a liquid nitrogen cooled MCT detector. A glass cell fitted with a prismatic CaF_2 window was used. Each single beam spectrum was computed after averaging 256 interferometer scans taken with 8 cm^{-1} resolution at different potentials in the range 0.2–0.9 V. The spectra are presented in the form of the reflectance ratio R/R_o of a single beam spectrum, R, obtained at a given potential and a reference spectrum, R_o, obtained at 0.2 V. Only *p*-polarized light was used.

2.4. *DEMS measurements*

A computer controlled quadrupole mass spectrometer, MKS Instruments was used for the DEMS measurements. Details of this method are given elsewhere [23, 25]. Briefly, the method allows the online detection of volatile and gaseous products of electrochemical reactions during the application of a potential scan. The electrochemical cell was constructed according to the principles described in [26].

In a typical DEMS experiment the current against potential curves (cyclic voltammograms (CVs)) are recorded simultaneously with the mass intensity vs. potential curves (mass spectrometric cyclic voltammograms (MSCVs)), for selected values of m/z (mass/charge) ion signals. The potential was cycled in the range 0.05–0.90 V and the scan rate was 0.01 V s^{-1}.

2.5. *Normalization procedure*

Taking as a common system the oxidative stripping of a saturated CO monolayer, normalization factors were calculated for each of the measured parameters. For this purpose the CO saturation coverages were achieved by bubbling CO for 5 min at 0.2 V followed by bubbling N_2 for 10 min in order to eliminate dissolved CO.

For the voltammetric currents of cyclic voltammograms we took the charge, Q_{ox}, (Figure 1(a)) necessary to oxidize a CO monolayer. For the mass spectrometry signals we integrated the corresponding signal, Q_m, for the CO_2 ($m/z = 44$) produced during CO stripping, as shown in Figure 1(b). Similarly, the IR band intensities were normalized using the integrated band intensity for the CO_2 produced after total oxidation of a saturated CO adlayer. In this case CO was adsorbed at 0.2 V and oxidized by applying a potential step to 0.7 V at which CO can be completely eliminated from the surface (spectra 2, 3 etc., of Figure 1(c)). Taking a sequence of 30 scan spectra, the band intensity for CO_2 (2341 cm^{-1}) increased, passing through a maximum value after about 30 s (spectrum 5, Figure 1(c)) and began to decrease slowly after about 60 s. These changes indicate that the complete oxidation of the CO monolayer requires a given time, which is probably longer due to the thin layer configuration in the IR experiment. Slow diffusion of CO_2 to the solution outside the thin layer causes a subsequent decrease in the band intensity. The maximum value for the integrated band intensity (as indicated in spectrum) was used as a normalization factor for the amount of CO_2 produced during alcohol oxidation [24].

All data were taken at room temperature. The values of the normalization factors obtained by the described methods are listed in Table 1.

3. Results and discussion

3.1. *DEMS results*

Cyclic voltammograms for methanol oxidation on electrodeposited Pt and PtRu are shown in Figure 2(a).

Table 1. Obtained normalization factors from the prepared electrodes

DEMS			FTIR	
Electrode compositions	Normalization factor for CVs (Q_{ox} value/C)	Normalization factor for MSCVs (Q_m value/10^{-11} C)	Electrode compositions	Normalization factor for IR band intensities/a.u.
Pt	0.0121	3.639	Pt	1.289
$Pt_{86}Ru_{14}$	0.0270	1.834	$Pt_{90}Ru_{10}$	6.369
$Pt_{75}Ru_{25}$	0.0173	0.7084	$Pt_{75}Ru_{25}$	3.506
$Pt_{65}Ru_{35}$	0.0163	0.9113	$Pt_{63}Ru_{37}$	7.062

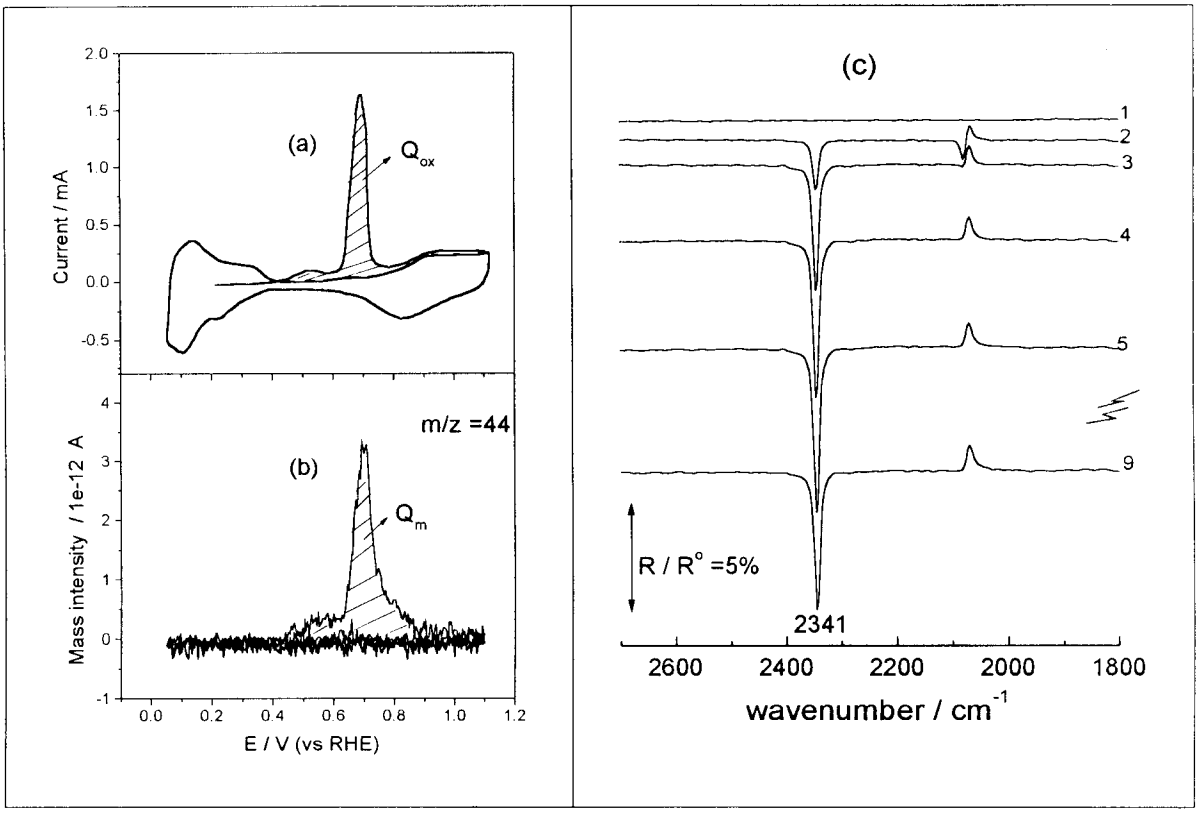

Fig. 1. Determination of normalization factors. (a) CV of CO oxidation on porous platinum (DEMS electrode) at 10 mV s^{-1}, showing the charge Q_{ox} obtained after oxidation of the saturated CO overlayer. (b) CV of online mass signals of CO oxidation as in Figure 1(a). The integrated signal Q_m serving as normalization factor. (c) FTIR spectra (base line corrected) of CO oxidation at deposited Pt on smooth gold in 0.1 M $HClO_4$ at different potentials and time (see text), the integrated intensity maximum of CO_2 was used as normalization factor.

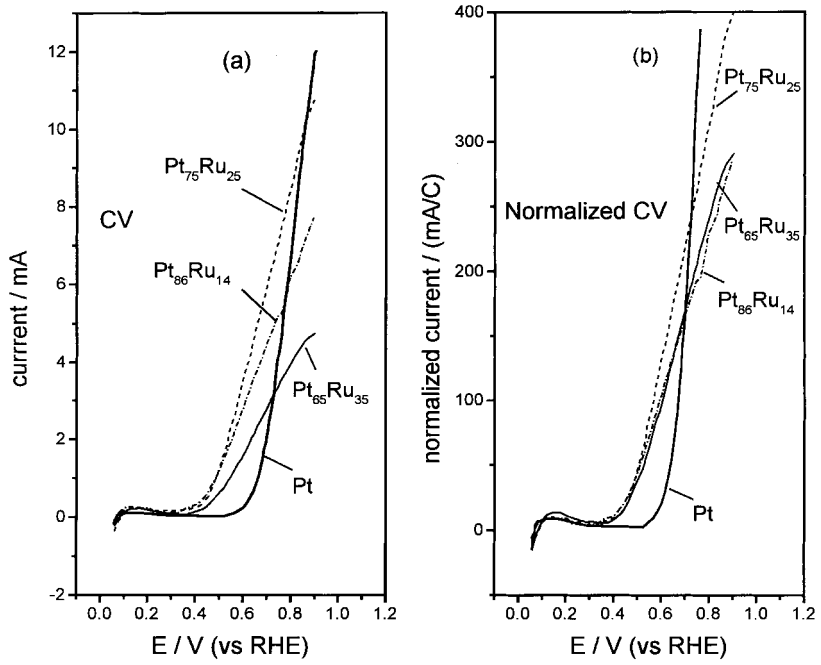

Fig. 2. Cyclic voltammograms of methanol oxidation at different PtRu electrodeposits on sputtered gold, 0.1 M CH_3OH in 0.1 M $HClO_4$, 10 mV s^{-1}, geometric surface 1.13 cm^2, (a) without normalization, (b) normalized as described in paragraph 2.5 (Figure 1(a)), dividing the current by the corresponding Q_{ox} value (Table 1).

The corresponding normalized CVs are shown in Figure 2(b). It is seen from the plots in Fig. 2a that the increasing order for the observed current in the potential range 0.4–0.6 V, is $Pt_{75}Ru_{25} > Pt_{86}Ru_{14} > Pt_{65}Ru_{35} >$ Pt. The normalized CVs in Figure 2(b) again exhibit the highest current data for $Pt_{75}Ru_{25}$, as in the case of the

not normalized data; however, the two other alloys have almost the same catalytic activity.

In Figure 3 the mass signals for CO_2 production during the potential scans of Figure 2 are shown. Considering that CO_2 is by far the main product of methanol eletrooxidation, it should be expected that the order of activities determined by the $m/z = 44$ signal and by the electrochemical currents are the same. However, a comparison of Figures 2(a) and 3(a) and Figures 2(b) and 3(b) shows that the same order of activities is achieved, *only* for normalized signal plots. The normalized plots of currents and mass intensity signals clearly agree with $Pt_{75}Ru_{25}$ being the best catalyst, the two other alloys showing, within the error of the measurements, about the same activity. These results indicate that the microstructure of the porous (DEMS) electrodes is an uncontrolled experimental parameter; it is an intrinsic property of each electrode. The specific structure determines the number of active sites per geometric surface and, therefore, the current. In the case of DEMS electrodes the mass signals are proportional to the electrochemical current [23, 25]; however, the proportionality factor is *not* the same for different electrodes. Even using the same procedure for electrode preparation, the final surface roughness and microporosity may differ from one electrode to the other. Also the composition and total amount of electrodeposited material may influence the porous structure of the electrode, thus affecting the permeability to the gaseous products. It is found experimentally, that the proportionality factor between current and mass response is an intrinsic property of the electrode. This is another reason for distinct normalization factors.

3.2. *FTIR results*

The potential dependence of the integrated band intensity for CO_2 production during methanol electrooxidation is given in Fig. 4a, b, without and with normalization, respectively. According to Figure 4(a) the $Pt_{90}Ru_{10}$ electrode presents the highest band intensities and is apparently the most active one, followed, in descending order, by the $Pt_{75}Ru_{25}$, $Pt_{63}Ru_{37}$ and Pt electrodes. This result does not agree with either the normalized or non-normalized data in the CV and MSCV experiments of Figures 2 and 3. The normalized IR data (Figure 4(b)) show that for the 0.3–0.6 V potential range the order of activities is $Pt_{75}Ru_{25} > Pt_{90}Ru_{10} > Pt_{63}Ru_{37} > Pt$. Above 0.7 V the Pt electrode becomes the most active one, as is already well known and also shown above by the CV and MSCV results.

These IR results are in good agreement with the order of electrode activities obtained from normalized CVs and MSCV data except for the fact that IR data show differences in the behaviour of $Pt_{90}Ru_{10}$ and $Pt_{63}Ru_{37}$, which are more pronounced than the differences shown by DEMS for $Pt_{86}Ru_{14}$ and $Pt_{65}Ru_{35}$ (Figures 2 and 3). Apart from differences in texture (see Section 2.1) and exact composition of the electrodes, DEMS and *in situ* FTIR present more significant differences. The comparison between the results of both methods can be done only with certain restrictions. IR spectra were collected over a period of about 1 min, during which the potential was held at a given value. Carbon dioxide produced at each potential is trapped in the cavity of the thin layer, thus producing an accumulation effect on spectra taken in a sequence of potential steps as in the present case. In

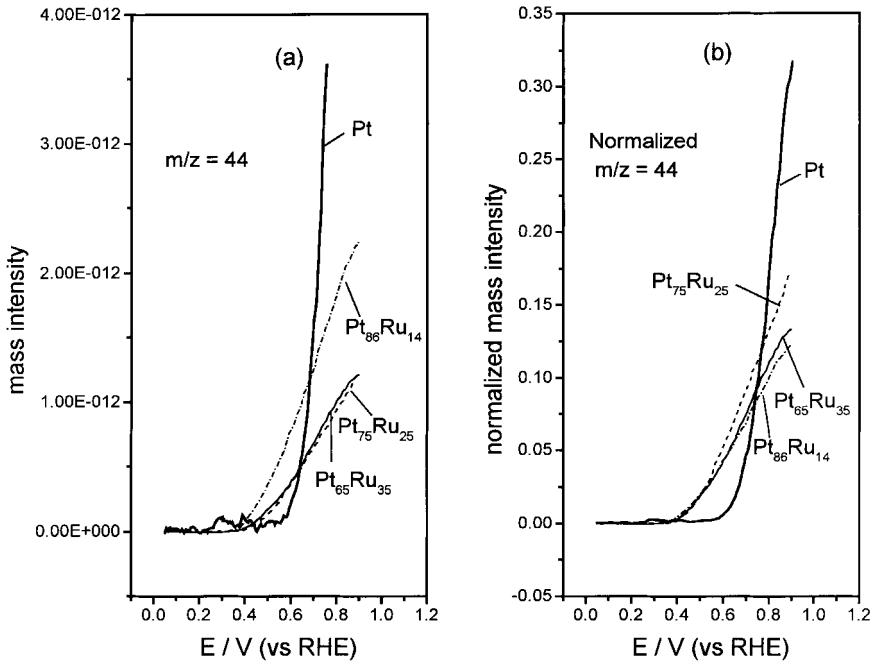

Fig. 3. Cyclic voltammograms of methanol oxidation as in Figure 2, but taking off online mass signals $m/z = 44$ using DEMS, (a) without normalization, (b) normalized as described in paragraph 2.5 (Figure 1(b)), dividing the mass intensities of Figure 3(a) by the values of Q_m. (Table 1).

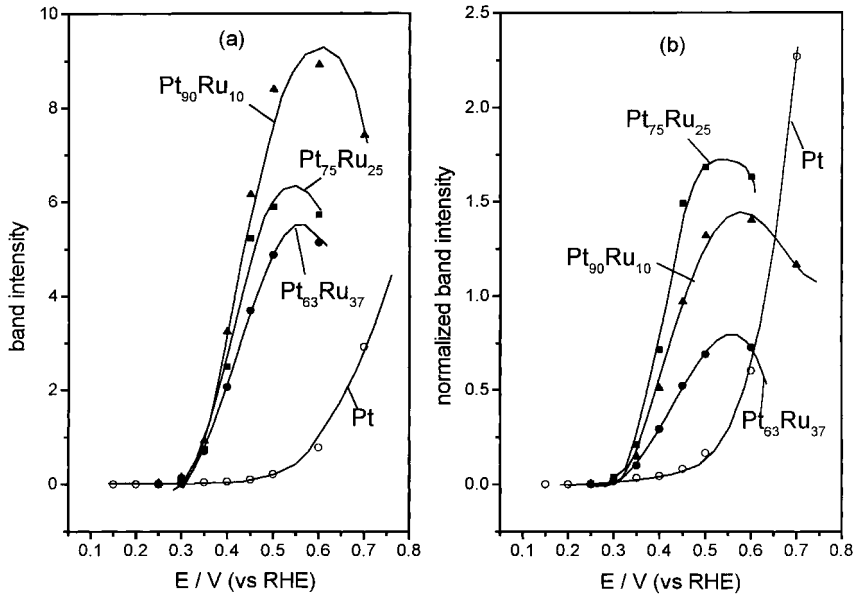

Fig. 4. Potential step voltammograms of integrated FTIR band intensities of CO_2 (ν = 2341 cm^{-1}) during methanol oxidation at different PtRu electrodeposits on a smooth gold surface. 0.1 M CH_3OH + 0.1 M $HClO_4$, 256 scans, 8 cm^{-1} resolution. (a) Without normalization, (b) with normalization according to paragraph 2.5 (Figure 1(c)).

contrast, during a DEMS experiment, CO_2 is continually pumped away, so that as the potential increases the MS response 'differentially' increases with the current. On the one hand, the mass signal is directly proportional to the number of molecules reaching the ion source. On the other hand, the reflectance ratio, R/R_o, for species in solution (as, in this case, CO_2), follows the Lambert–Beer law, thus being an exponential function of the CO_2 concentration. This explains the better resolution of FTIR as compared to DEMS.

In summary, the normalized plots show that at room temperature from all electrodes tested here, the one with 25% Ru bulk composition has the highest electrocatalytic activity in the potential range 0.4–0.6 V, the Pt electrode being the best above 0.7 V. As shown by Gasteiger et al. [27], in addition to atomic distribution, temperature and methanol concentration do also affect the position of the maximum in respect to PtRu composition. Using UHV well prepared alloys, experimental data with a high activity near the above PtRu composition have been reported [27, 28]. In this case normalization based on the geometric area of the electrode alone is acceptable.

Nevertheless, a word of caution is necessary. When comparing activity data of 'deposits' and 'alloys', it has to be considered that the atomic surface distribution for a given PtRu composition may be quite different for the two metal surfaces. This can have an influence on the reaction rate and, therefore, also on the position of the maximum in the plot of activity versus PtRu composition.

4. Conclusion

Monitoring different responses such as current, MS signals and FTIR band intensities make it possible to follow the rate of reactions, as in the present example methanol oxidation at porous PtRu layers. The results obtained agree very well for the three methods used only if the data are normalized to the active real surface of the electrodes. As a normalization procedure for the study of Pt-based porous catalysts, the oxidative stripping of a CO layer at saturated coverage seems to be very suitable.

Acknowledgements

Financial support by the Deutsche Forschungsgemeinschaft, CAPES, CNPq and FAPESP is gratefully acknowledged. J.P.I.S. acknowledges Bundeswehr University Munich for financial support during his stay.

References

1. J. Clavilier, C. Lamy and J.M. Leger, *J. Electroanal. Chem.* **125** (1981) 249.
2. X.H. Xia, T. Iwasita, F. Ge and W. Vielstich, *Electrochim. Acta* **41** (1996) 711.
3. H.A. Gasteiger, N. Markovic, P.N. Ross and E.J. Cairns, *J. Phys. Chem.* **97** (1993) 12020.
4. H.A. Gasteiger, N. Markovic and P.N. Ross, *J. Phys. Chem.* **99** (1995) 8290.
5. M. Wakizoe, O.A. Velev and S. Srinivasan, *Electrochim. Acta* **40** (1995) 335.
6. V.A. Paganin, E.A. Ticianelli and E.R. Gonzales, *J. Appl. Electrochem.* **26** (1996) 297.
7. M. Watanabe and S. Motoo, *J. Electroanal. Chem.* **60** (1975) 267.
8. A.K. Shukla, M.K. Ravikumar, A.S. Ariko, G. Candiano, V. Atonucci, N. Giordano and A. Hamnett, *J. Appl. Electrochem.* **25** (1995) 528
9. S. Mukerjee, S.J. Lee, E.A. Ticianelli, J. McBreen, B.N. Grgur, N. Markovic, P.N. Ross, J.R. Giallombardo and E.S. De Castro, *ESS Lett.* **2** (1999) 12.
10. D. Chu and S. Gilman, *J. Electrochem. Soc.* **143** (1996) 1685.

11. M. Watanabe, M. Uchida and S. Motoo, *J. Electroanal. Chem.* **229** (1987) 395.
12. M. Krausa and W. Vielstich, *J. Electroanal. Chem.* **379** (1994) 307.
13. J.P.I. Souza, J.F.B. Rabelo, I.R. Moraes and F.C. Nart, *J. Electroanal. Chem.* **420** (1997) 17.
14. D.F.A. Koch, D.A.J. Rand and R. Woods, *J. Electroanal. Chem.* **70** (1976) 73.
15. J.P.I. Souza, S. Linhares and F.C. Nart, *J. Braz. Chem. Soc.*, submitted.
16. M.M.P. Janssen and J. Mulhuysen, *Electrochim. Acta* **21** (1976) 861.
17. P.K. Shen and A.C.C. Tsung, *J. Electrochem. Soc.* **141** (1994) 3082.
18. B.N. Grgur, G. Zhuang, N. Markovic and P.N. Ross, *J. Phys. Chem.* **101** (1997) 3910.
19. B.N. Grgur, N. Markovic and P.N. Ross, *J. Phys. Chem.* **102** (1998) 2494.
20. A. Hamnett and B.J. Kennedy, *Electrochim. Acta* **33** (1988) 1613.
21. R. Liu, K. Triantafillou, L. Liu, C. Pu, C. Smith and S. Smotkin, *J. Electrochem. Soc.* **44** (1997) 148.
22. P. Stonehart, *US Patent 5 208 207*, May 4 (1993).
23. O. Wolter, C. Giordano, F. Heitbaum and W. Vielstich, *J. Electrochem. Soc.* **128** (1981) C 130; Proc. Symp. Electrocatalysis, The Electrochem. Soc., Pennington, N.J. 1982, p. 235.
24. N.F. Lin, T. Iwasita and W. Vielstich, *J. Phys. Chem.*, B **103** (1999) 3250.
25. B. Bittins-Cattaneo, E. Cattaneo, P. Königshoven and W. Vielstich, *in* A.J. Bard (Ed), '*Electroanalytical Chemistry – A Series of Advances', Vol* 17, (Marcel Dekker, New York, 1991) p. 181.
26. R. Ianniello and V.M. Schmidt, *Ber. Bunsenges Phys. Chem.* **99** (1995) 83.
27. H.A. Gasteiger, N. Markovic, P.N. Ross and E.J. Cairns, *J. Electrochem. Soc.* **141** (1994) 1795.
28. T. Iwasita, H. Hoster, A. John-Anacker, W.F. Lin and W. Vielstich, *Langmuir*, in press.